

Commensurate $(C_6H_{14}N_2)_2[Mo_8O_{26}] \cdot 4H_2O$ and incommensurate $(C_6H_{14}N_2)_2[Mo_8O_{26}] \cdot 4.66H_2O$: a structural versatility linked to solvent content

Michel Evain,^{a*} Vaclav Petricek,^b
Violaine Coué,^a Rémi Dessapt,^a
Martine Bujoli-Doeuff^a and
Stéphane Jobic^a

^aLaboratoire de Chimie des Solides, IMN, UMR 6502 CNRS – Université de Nantes, 2 rue de la Houssinière, BP 32229, 44322 Nantes CEDEX 3, France, and ^bInstitute of Physics, Academy of Sciences of the Czech Republic, Na Slovance 2, 182 21 Praha 8, Czech Republic

Correspondence e-mail:
michel.evain@cnrs-imn.fr

Received 24 April 2006

Accepted 4 July 2006

The syntheses and structure determinations by means of single-crystal X-ray diffraction of commensurate $(C_6H_{14}N_2)_2[Mo_8O_{26}] \cdot 4H_2O$ and incommensurate $(C_6H_{14}N_2)_2[Mo_8O_{26}] \cdot 4.66H_2O$, two new organic–inorganic hybrid compounds based on polyoxomolybdates and differing in their solvent content, are reported. Given the important disorder observed in the latter compound, only a combination of non-harmonic waves, crenel functions and TLS tensors offered a good modelling of the structure. $(C_6H_{14}N_2)_2[Mo_8O_{26}] \cdot nH_2O$ results from the self-assembly of $[Mo_8O_{26}]^{4-}$ anionic chains, $C_6H_{14}N_2^{2+}$ (H_2DABCO^{2+}) cations and water molecules. The $[Mo_8O_{26}]^{4-}$ chain is built from γ - $[Mo_8O_{28}]^{8-}$ octamolybdate clusters, connected to each other through corner sharing. In both compounds, the $[Mo_8O_{26}]^{4-}$ chains are separated, in a similar way, by the H_2DABCO^{2+} subunits, acting as charge-compensating cations, and by the water molecules. The orientation of the H_2DABCO^{2+} cations is shown to be different from what has been observed previously in monoclinic $(H_2DABCO)_2[Mo_8O_{26}] \cdot 4H_2O$, and therefore to give a different network of hydrogen bonds.

1. Introduction

In the past few years, organic–inorganic hybrid materials based on polyoxometalates (POMs) have received much attention in relation to their potential applications in catalysis (Mizuno & Misono, 1998), medicine (Rhule *et al.*, 1998) and optics (Katsoulis, 1998). Specifically, organoammonium salts of POMs exhibit all the requisites to generate photochromic properties owing to the ability of the organic component to return a proton to the mineral part under light illumination, with a concomitant reduction of Mo^{VI} species into Mo^V and stabilization of a metastable thermodynamic state (Yamase, 1998).

In the course of a study on 1,4-diazabicyclo[2.2.2]octane ($C_6H_{12}N_2$, DABCO) and Mo(POMs) (Coué *et al.*, 2006), two new, similar compounds have been obtained: $(H_2DABCO)_2[Mo_8O_{26}] \cdot 4H_2O$, (I), and $(H_2DABCO)_2[Mo_8O_{26}] \cdot 4.66H_2O$, (II). The structure of the former compound is commensurate, while that of the latter is incommensurately modulated. Both structures are related to, but differ from, the monoclinic $(H_2DABCO)_2[Mo_8O_{26}] \cdot 4H_2O$, (III), reported by Fang *et al.* (2004). The three structures contain infinite $[Mo_8O_{26}]^{4-}$ anionic chains, as observed in $(C_4H_{14}N_2)_2[Mo_8O_{26}] \cdot 2H_2O$ (Thorn *et al.*, 2005) and $[H_3N(CH_2)_3NH_3]_2[Mo_8O_{26}] \cdot H_2O$ (Chakrabarti & Natarajan, 2002). Although none of them exhibit photochromism, the three compounds (I), (II) and (III) are interesting in demonstrating the flexibility of the interactions between the mineral chains and the H_2DABCO^{2+}

cations, either directly through hydrogen bonds or indirectly *via* water molecules.

In this paper we report the syntheses and the structure determinations of (I) and (II). The structure model of the incommensurate structure of (II) could not be found without the knowledge of the three-dimensional structure of (I) and required the use of rigid bodies, crenel functions and TLS tensors. The two new structures are analysed and compared with the structure of (III).

2. Synthesis

DABCO ($C_6H_{12}N_2$) was purchased from Aldrich and MoO_3 (99.95%) from Alfa Aesar. These materials were used without further purification. MoO_3 (720 mg, 5 mmol) was dispersed in 15 ml of water. DABCO (200 mg, 1.75 mmol) was then added to the solution. After a few minutes of stirring, 1 M HCl was added to adjust the pH to around 2.8. The mixture was sealed hydrothermally in a 30 ml Teflon-lined autoclave (453 K, 5 d, autogenous pressure). Blue–grey powder (remaining MoO_3) and colourless crystals were obtained. After filtration, the sample was dispersed in water and crystals were separated from the powder with ultrasonic waves before washing first in EtOH and then in Et_2O . Crystals consist of $(H_2DABCO)_2 \cdot [Mo_8O_{26}] \cdot xH_2O$, not modulated ($x = 4$) and modulated ($x = 4.66$).

3. Structure determination

3.1. Commensurate $(H_2DABCO)_2[Mo_8O_{26}] \cdot 4H_2O$, (I)

A single crystal of (I) suitable for data collection was found serendipitously in a large batch of crystals when looking for additional crystals of the incommensurate compound (II) (see below). Glued at the tip of a Lindemann capillary by means of a solvent-free glue, the chosen crystal was aligned on a Bruker–Nonius KappaCCD diffractometer. Preliminary lattice parameters and an orientation matrix were obtained from four sets of frames and refined when the intensity data were integrated. Intensity measurements were performed at 293 K using graphite-monochromated Mo $K\text{-}L_{2,3}$ radiation from a sealed tube. Data were processed using the Bruker–Nonius *EvalCCD* program package (Duisenberg *et al.*, 2003). Subsequent calculations were conducted with the *JANA2000* program suite (Petricek *et al.*, 2000), except for the crystal-shape and dimension optimization, which was performed with *X-SHAPE* (Stoe & Cie, 1996) based on the *HABITUS* program (Herrendorf, 1993), the structure solution, which was carried out with *SIR2004* (Burla *et al.*, 2005), and the structure drawings, which were realized with the *DIAMOND* program (Brandenburg, 2001).

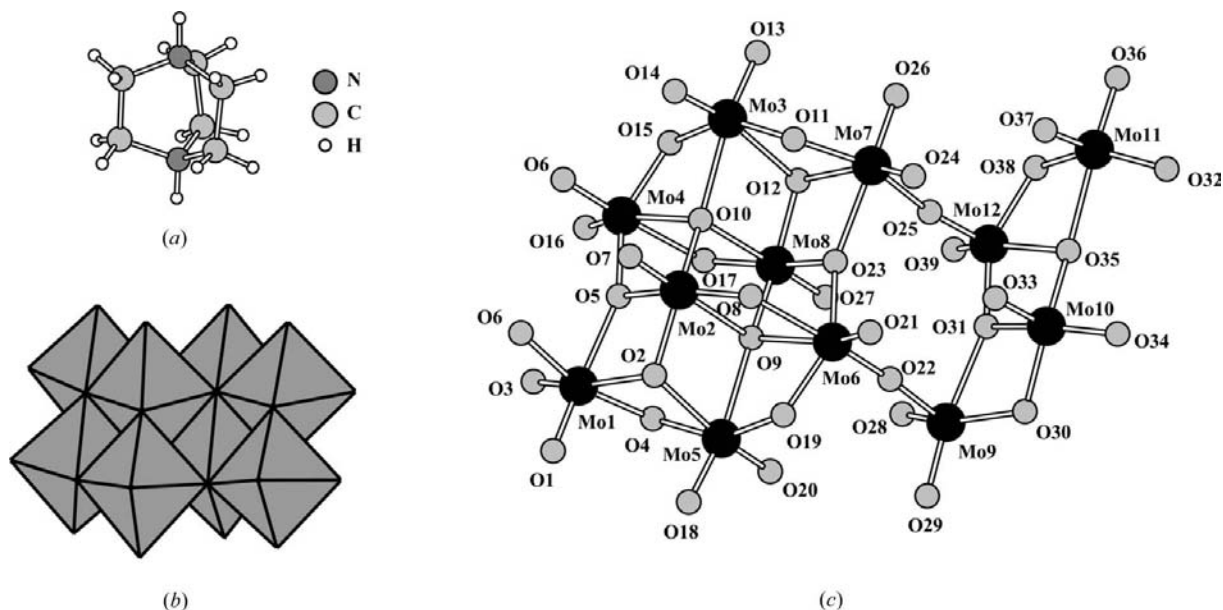
After absorption correction (Gaussian integration) and the averaging of symmetry-equivalent reflections ($\bar{1}$ point group), an initial structure solution with direct methods was found using *SIR2004*. The partial solution (the complete molybdate chain and part of the H_2DABCO entities) was easily completed through difference-Fourier map synthesis calcula-

Table 1
Experimental details.

	(I)	(II)
Crystal data		
Chemical formula	$(C_6H_{14}N_2)_2[Mo_8O_{26}] \cdot 4H_2O$	$(C_6H_{14}N_2)_2[Mo_8O_{26}] \cdot 4.66H_2O$
M_r	1483.9	1495.8
Cell setting, space group	Triclinic, $P\bar{1}$	Triclinic, $P\bar{1}(\alpha\beta\gamma)0$
Temperature (K)	293	293
a, b, c (Å)	12.3378 (15), 14.417 (2), 16.1439 (16)	7.8907 (5), 10.0855 (3), 12.4131 (8)
α, β, γ (°)	100.927 (9), 106.487 (8), 104.110 (10)	113.685 (4), 92.857 (7), 101.244 (5)
V (Å ³)	2565.0 (6)	878.20 (9)
q	–	0.0633 (3) a * – 0.4284 (5) b * – 0.4159 (6) c *
Z	3	1
D_x (Mg m ⁻³)	2.881	2.828
Radiation type	Mo $K\alpha$	Mo $K\alpha$
μ (mm ⁻¹)	2.95	2.87
Crystal form, colour	Elongated block, colourless	Elongated block, colourless
Crystal size (mm)	0.18 × 0.10 × 0.08	0.24 × 0.10 × 0.08
Data collection		
Diffractometer	Bruker–Nonius KappaCCD	Bruker–Nonius KappaCCD
Data collection method	ω scans	φ and ω scans
Absorption correction	Gaussian	Gaussian
T_{\min}	0.595	0.649
T_{\max}	0.833	0.826
No. of measured, independent and observed reflections	90 290, 21 895, 14 316	153 057, 39 145, 21 512
Criterion for observed reflections	$I > 2\sigma(I)$	$I > 2\sigma(I)$
R_{int}	0.068	0.064
θ_{\max} (°)	35.0	35.9
Refinement		
Refinement on	F^2	F^2
$R[F^2 > 2\sigma(F^2)],$ $wR(F^2), S$	0.058, 0.135, 1.43	0.052, 0.133, 1.34
No. of reflections	21 895 reflections	39 145 reflections
No. of parameters	730	566
H-atom treatment	Constrained to parent site	Constrained to parent site
Weighting scheme	$w = 1/[\sigma^2(I) +$ $0.001936I^2]$	$w = 1/[\sigma^2(I) +$ $0.001936I^2]$
$(\Delta/\sigma)_{\max}$	0.001	0.002
$\Delta\rho_{\max}, \Delta\rho_{\min}$ (e Å ⁻³)	1.61, –1.89	2.11, –1.88

Computer programs used: *EvalCCD* (Duisenberg *et al.*, 2003), *JANA2000* (Petricek *et al.*, 2000), *X-SHAPE* (Stoe & Cie, 1996), *HABITUS* (Herrendorf, 1993), *SIR2004* (Burla *et al.*, 2005), *DIAMOND* (Brandenburg, 2001).

tions. From geometry considerations and to fulfil the overall charge balance, lone atoms were assigned as O atoms. H atoms were positioned geometrically for the three independent H_2DABCO entities and included in the refinement in the riding-model approximation with atomic displacement parameters equal to $1.2U_{\text{eq}}$ of the corresponding carrier atom. The H atoms of the six water molecules could not be found in the difference-Fourier syntheses. Therefore, since they could not be unambiguously located from the overall hydrogen-bond network, they were omitted. Crystal characteristics, data


Figure 1

(a) The $\text{H}_2\text{DABCO}^{2+}$ ($\text{C}_6\text{H}_{14}\text{N}_2^{2+}$) cation. (b) The $[\text{Mo}_8\text{O}_{26}]^{8-}$ γ -octamolybdate cluster. (c) The symmetry-independent molybdate entity [except for O6, which occurs two times, the lower atom at $(1-x, 1-y, -z)$], showing the self-aggregation of the γ -octamolybdate entities through μ_2 -O (O22 and O25) corner sharing.

collection and reduction parameters, and refinement results are gathered in Table 1.¹

3.2. Incommensurate $(\text{H}_2\text{DABCO})_2[\text{Mo}_8\text{O}_{26}] \cdot 4.66\text{H}_2\text{O}$, (II)

A single crystal of (II) was selected from the large number of crystals prior to the finding of the commensurate compound (I). The crystal of (II) was secured at the tip of a Lindemann capillary by means of solvent-free glue. A preliminary analysis on a Bruker–Nonius KappaCCD diffractometer clearly revealed a basic triclinic cell with additional weaker reflections, which could be indexed as satellites with $\mathbf{q} \simeq 0.06\mathbf{a}^* - 0.42\mathbf{b}^* - 0.42\mathbf{c}^*$. A data collection was carried out at room temperature on the KappaCCD diffractometer, using two different exposure times because some reflections were so much stronger than others and a $\sin(\theta)/\lambda = 0.83$ cutoff ($\theta_{\max} = 36^\circ$). In addition, to prevent partial overlapping of satellites, a longer detector distance [72 mm instead of 25.2 mm for (I)] and a smaller scan angle [0.3° instead of 1.9° for (I)] were chosen. The lattice parameters were post-refined (Evain, 1992) from the positions of 985 reflections obtained with the diffractometer and a $(3+1)$ -dimensional indexing: $a_s = 7.8907$ (5), $b_s = 10.0855$ (3), $c_s = 12.4131$ (8) Å, $\alpha_s = 113.685$ (4), $\beta_s = 92.857$ (7), $\gamma_s = 101.244$ (5)°, $\mathbf{q} = 0.0633$ (3) $\mathbf{a}^* - 0.4284$ (5) $\mathbf{b}^* - 0.4159$ (6) \mathbf{c}^* , and $V_s = 878.20$ (9) Å³ ($Z = 1$). Data collection details are gathered in Table 1.

The intensity integration was carried out with *EvalCCD*. The set of reflection intensities was then corrected for absorption *via* a Gaussian analytical method, after dimension optimization with *X-SHAPE*. Symmetry-equivalent reflec-

tions were then merged according to the $(\bar{1}, \bar{1})$ $(3+1)$ -dimensional point group, with residual value $R_{\text{int}} = 0.055$ [$I \geq 2\sigma(I)$ cutoff, average redundancy of 3.91]. A set of 39 145 independent reflections (21 512 observed with 6655 main + 10 636 first order + 4221 second order) were then available for refinement.

A partial solution for the average structure was found in the $P\bar{1}$ space group with the direct methods of *SIR2004*. That solution included an $[\text{Mo}_4\text{O}_{13}]$ molybdate fragment, yielding chains running along the a axis, and a few additional atoms without an obvious link to H_2DABCO entities. However, working with Fourier and difference-Fourier maps, a group of atoms approximating H_2DABCO in shape and with very large atomic displacement parameters could be positioned, along with two isolated atoms corresponding to water molecules. Using that solution as a starting point, the refinement was then carried out in the $(3+1)$ -dimensional superspace with the $P\bar{1}(\alpha\beta\gamma)0$ superspace group. The agreement could be improved by introducing displacive modulation parameters for Mo and O atoms of the molybdate entity, but no real improvement could be achieved with the organic part of the structure.

At that stage it was decided to look for another crystal, which led to the finding of the commensurate compound (I) and the determination of its structure (see above). With that solution in hand, it was realized that differently oriented $\text{H}_2\text{DABCO}^{2+}$ cations were overlapping in the average structure and that they could not be easily modelled with displacive waves (see structure description). The $\text{H}_2\text{DABCO}^{2+}$ cation was then introduced in the refinement as a rigid body in two different orientations, with occupations in the internal t space modelled by the setting of complementary crenel functions (Petricek *et al.*, 1995). Concurrently, it was realized that, out of

¹ Supplementary data for this paper are available from the IUCr electronic archives (Reference: SN5039). Services for accessing these data are described at the back of the journal.

the three water molecules, two were not defined over the periodicity of the internal space and that their occupation was correlated to the $\text{H}_2\text{DABCO}^{2+}$ cation orientation. For a proper description of the site occupation factors, crenel functions were then introduced for those two molecules. With large crenel domains, no orthogonalization procedure was required for the refinement stability. The occupation of the third water molecule was, on the other hand, modulated through standard harmonic functions without any domain restriction within the internal space.

With the overall structure organization thus defined, the refinement converged smoothly through the successive introduction of displacive modulation functions and modulation functions for the anisotropic ADPs for Mo atoms. Various attempts were then carried out for a good modelling of the $\text{H}_2\text{DABCO}^{2+}$ cation position and orientation. Only the introduction of TLS tensors for both complementary defined cations gave satisfactory refinements, one of the two differently oriented $\text{H}_2\text{DABCO}^{2+}$ cations being rotationally disordered (see structure description). Crystal characteristics, data collection and reduction parameters, and refinement results are gathered in Table 1, and final residual factors in Table 2. Atomic parameters are reported in Tables 3–5.

4. Structure description

4.1. Commensurate $(\text{H}_2\text{DABCO})_2[\text{Mo}_8\text{O}_{26}]\cdot 4\text{H}_2\text{O}$, (I)

Compound (I) results from the self-assembly of $[\text{Mo}_8\text{O}_{26}]^{4-}$ anionic chains, $\text{H}_2\text{DABCO}^{2+}$ cations (Fig. 1*a*) and water molecules. The $[\text{Mo}_8\text{O}_{26}]^{4-}$ chain is built from $\gamma\text{-}[\text{Mo}_8\text{O}_{28}]^{8-}$ octamolybdate clusters, as depicted in Fig. 1*b*), connected to each other through corner sharing (Fig. 1*c*). Within the clusters, Mo atoms occupy distorted octahedra with comparable geometry, *i.e.* two shorter, two medium and two longer bond distances realized with $\mu_1\text{-O}$, $\mu_2\text{-O}$ and $\mu_3\text{-O}$, respectively. The average Mo–O distance ranges from 1.946 to 1.973 Å for the 12 independent Mo atoms. This octamolybdate chain arrangement is identical to that found in (III) (Fang *et al.*, 2004).

In compounds (I) and (III), the $[\text{Mo}_8\text{O}_{26}]^{4-}$ chains are separated, in a similar way, by the $\text{H}_2\text{DABCO}^{2+}$ subunits, acting as charge-compensating cations, and by the water molecules (see Figs. 2*a* and 2*b*, respectively). However, as is clearly seen in Figs. 2*a*) and 2*b*), there exist two different orientations of the $[\text{Mo}_8\text{O}_{26}]^{4-}$ chains for compound (III) but only one for compound (I). In addition to that difference, the striking difference between the two structures is the different orientation of the $\text{H}_2\text{DABCO}^{2+}$ cations and thus the different network of hydrogen-bond interactions (see Figs. 3*a* and 3*b*). In compound (III), the $\text{H}_2\text{DABCO}^{2+}$ cations are linked through hydrogen bonds only to the water molecules, which establish the link with the POM anionic chains. If, in compound (I), two out of the three independent $\text{H}_2\text{DABCO}^{2+}$ cations are also ‘parallel’ to the inorganic anionic chains and establish hydrogen bonds exclusively with water molecules, one $\text{H}_2\text{DABCO}^{2+}$ cation is ‘perpendicular’ to the chains and

Table 2

Final residual factors for (II).

	<i>N</i> (obs)	<i>R</i> (obs)	<i>R_w</i> (obs)
Overall	21512	0.0517	0.1194
Main	6655	0.0344	0.0912
First order	10636	0.0566	0.1207
Second order	4221	0.1416	0.2657

directly connects those chains. As a result, some water molecules of (I) do not have any connection to the $\text{H}_2\text{DABCO}^{2+}$ cations and are only linked to the chains and/or to the other water molecules.

It is worth noting that the structure of (I) could have been described as a commensurately modulated structure, with the basic structure of incommensurate (II). This approach has not been considered in the present study since it would have required, as for compound (II), the use of superspace and crenel functions for a proper description of the $\text{H}_2\text{DABCO}^{2+}$ cation orientation, which would have unnecessarily complicated its structure analysis and visualization.

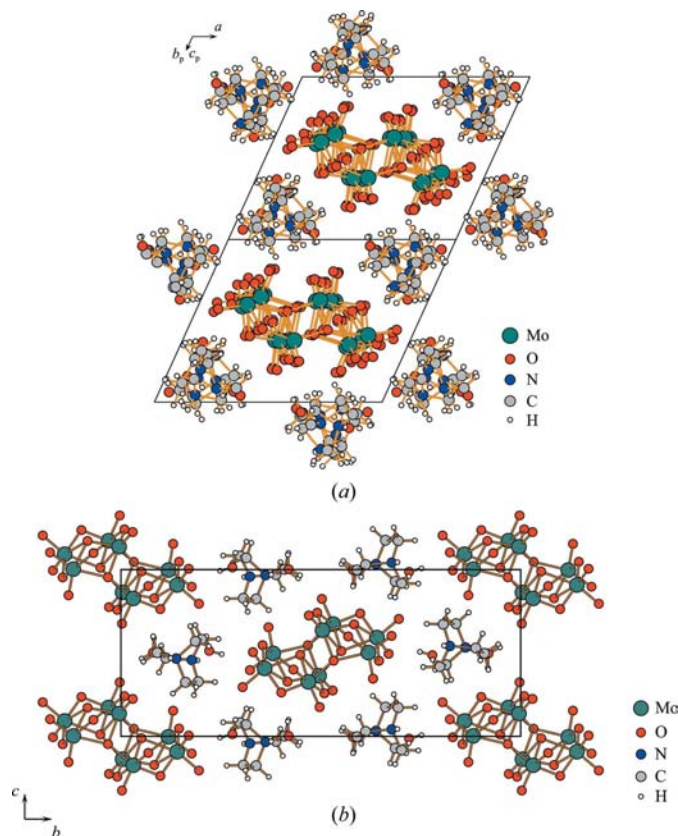


Figure 2

(*a*) View along the $[01\bar{1}]$ axis (*b* and *c* axes are therefore projected onto the view plane) of the structure of (I), showing the polyoxometalate anionic chains separated by the $\text{H}_2\text{DABCO}^{2+}$ cations and the water molecules. (*b*) Projection along the $[100]$ axis of the structure of (III) (Fang *et al.*, 2004), illustrating the two different orientations of the polyoxometalate chains and the parallel-like alignment of the $\text{H}_2\text{DABCO}^{2+}$ cations with the chains.

Table 3

Fractional atomic coordinates, their Fourier series modulation terms, equivalent isotropic displacement parameters (\AA^2) and s.u. values for (II).

The f modulation wave for a parameter λ of an atom v is classically written as

$$f_{\lambda}^v(x_4) = f_{\lambda,0}^v + \sum_{n=1}^k f_{\lambda,s,n}^v \sin(2\pi n x_4) + \sum_{n=1}^k f_{\lambda,c,n}^v \cos(2\pi n x_4).$$

Atom	n	x	y	z	U_{eq}
Mo1		0.01475 (2)	0.10641 (2)	0.793165 (14)	0.01834 (6)
s,1		0.00173 (3)	-0.01539 (3)	0.00305 (2)	
c,1		0.01299 (3)	0.02001 (3)	0.01094 (2)	
s,2		-0.00261 (5)	-0.00121 (4)	0.00154 (3)	
c,2		0.00081 (5)	-0.00031 (4)	-0.00233 (3)	
s,3		0.00161 (11)	0.00131 (7)	0.00391 (6)	
c,3		0.00152 (11)	0.00709 (7)	-0.00063 (6)	
Mo2		0.41800 (2)	0.149828 (18)	0.739826 (14)	0.01804 (5)
s,1		0.00311 (3)	-0.00520 (2)	0.006949 (19)	
c,1		0.01297 (3)	0.01608 (3)	0.00942 (2)	
s,2		-0.00158 (5)	-0.00037 (4)	0.00187 (3)	
c,2		0.00137 (5)	0.00030 (4)	-0.00234 (3)	
s,3		0.00096 (13)	0.00126 (9)	0.00215 (7)	
c,3		0.00190 (13)	0.00324 (9)	-0.00103 (7)	
Mo3		0.304037 (18)	0.117739 (17)	0.419560 (14)	0.01527 (5)
s,1		0.01086 (3)	0.01121 (2)	0.01144 (2)	
c,1		-0.00328 (3)	-0.00814 (2)	-0.006788 (18)	
s,2		0.00181 (4)	0.00052 (4)	-0.00295 (3)	
c,2		-0.00048 (4)	-0.00053 (4)	-0.00077 (3)	
s,3		0.00116 (14)	-0.00132 (11)	-0.00338 (8)	
c,3		-0.00084 (14)	0.00135 (10)	0.00063 (8)	
Mo4		-0.114145 (19)	0.118717 (16)	0.480196 (13)	0.01409 (5)
s,1		0.01207 (3)	0.01270 (2)	0.013123 (19)	
c,1		0.00040 (3)	-0.00370 (2)	-0.004949 (18)	
s,2		0.00152 (4)	0.00067 (3)	-0.00231 (3)	
c,2		0.00112 (4)	0.00023 (3)	-0.00144 (3)	
s,3		0.00173 (13)	-0.00088 (10)	-0.00306 (7)	
c,3		-0.00086 (13)	-0.00032 (10)	-0.00157 (7)	
O1		-0.06329 (17)	0.05779 (15)	0.60558 (12)	0.0165 (4)
s,1		0.0095 (2)	0.00797 (19)	0.01190 (16)	
c,1		0.0056 (2)	0.01093 (19)	0.00426 (15)	
s,2		0.0008 (3)	0.0005 (3)	-0.0020 (2)	
c,2		0.0013 (3)	0.0007 (3)	-0.0022 (2)	
O2		-0.1051 (2)	0.2348 (2)	0.84722 (16)	0.0333 (6)
s,1		-0.0048 (3)	-0.0262 (3)	0.0086 (2)	
c,1		0.0127 (3)	0.0096 (3)	0.0142 (2)	
s,2		-0.0010 (5)	0.0007 (4)	0.0029 (3)	
c,2		-0.0032 (5)	-0.0024 (4)	0.0009 (3)	
O3		-0.17194 (18)	-0.08043 (17)	0.72417 (13)	0.0206 (5)
s,1		0.0078 (2)	-0.0001 (2)	0.00542 (17)	
c,1		0.0098 (2)	0.0243 (2)	0.01429 (17)	
s,2		-0.0006 (4)	-0.0022 (3)	-0.0030 (2)	
c,2		0.0029 (4)	0.0019 (3)	-0.0021 (2)	
O4		0.0839 (2)	0.0760 (2)	0.91185 (15)	0.0317 (6)
s,1		0.0044 (3)	-0.0345 (3)	-0.0073 (2)	
c,1		0.0123 (3)	0.0182 (3)	0.0129 (2)	
s,2		-0.0043 (4)	-0.0022 (4)	0.0023 (3)	
c,2		-0.0002 (5)	-0.0040 (4)	-0.0027 (3)	
O5		0.18520 (18)	-0.04563 (16)	0.68331 (12)	0.0185 (4)
s,1		0.0105 (2)	0.0033 (2)	0.00746 (16)	
c,1		0.0080 (2)	0.0223 (2)	0.01257 (16)	
s,2		0.0004 (4)	-0.0005 (3)	-0.0026 (2)	
c,2		0.0014 (4)	0.0009 (3)	-0.0016 (2)	
O6		0.22161 (19)	0.23677 (16)	0.78452 (13)	0.0218 (5)
s,1		-0.0018 (3)	-0.0153 (2)	0.00607 (18)	
c,1		0.0133 (3)	0.0148 (2)	0.01106 (18)	
s,2		-0.0026 (4)	-0.0013 (3)	0.0036 (2)	
c,2		-0.0014 (4)	-0.0003 (3)	-0.0012 (2)	
O7		0.4736 (2)	0.1296 (2)	0.86514 (15)	0.0343 (7)
s,1		-0.0039 (3)	-0.0217 (3)	-0.0003 (2)	

Table 3 (continued)

Atom	n	x	y	z	U_{eq}
c,1		0.0153 (3)	0.0219 (3)	0.0136 (2)	
s,2		-0.0014 (5)	0.0022 (4)	0.0046 (3)	
c,2		-0.0011 (5)	0.0004 (4)	-0.0017 (3)	
O8		0.55103 (18)	-0.00333 (17)	0.64663 (13)	0.0233 (5)
s,1		0.0098 (2)	0.0066 (2)	0.00990 (18)	
c,1		0.0054 (2)	0.0122 (2)	0.00748 (18)	
s,2		0.0003 (4)	-0.0004 (3)	-0.0018 (3)	
c,2		0.0013 (4)	0.0000 (3)	-0.0027 (3)	
O9		0.5569 (2)	0.30712 (19)	0.75102 (17)	0.0328 (6)
s,1		0.0003 (3)	-0.0082 (2)	0.0109 (2)	
c,1		0.0128 (3)	0.0118 (2)	0.0085 (2)	
s,2		-0.0024 (4)	-0.0004 (4)	0.0029 (3)	
c,2		-0.0001 (4)	0.0007 (4)	-0.0005 (3)	
O10		0.30421 (17)	0.08414 (15)	0.55868 (12)	0.0179 (4)
s,1		0.0107 (2)	0.00922 (19)	0.01162 (16)	
c,1		0.0039 (2)	0.00840 (19)	0.00156 (16)	
s,2		0.0019 (3)	0.0004 (3)	-0.0019 (2)	
c,2		0.0011 (3)	0.0004 (3)	-0.0020 (2)	
O11		0.4254 (2)	0.29384 (18)	0.46168 (15)	0.0260 (5)
s,1		0.0136 (3)	0.0141 (2)	0.0172 (2)	
c,1		-0.0016 (3)	-0.0017 (2)	-0.0073 (2)	
s,2		0.0016 (4)	0.0015 (3)	-0.0005 (3)	
c,2		0.0014 (4)	0.0006 (3)	-0.0039 (3)	
O12		0.09476 (18)	0.23147 (16)	0.49390 (13)	0.0205 (5)
s,1		0.0125 (2)	0.0138 (2)	0.01749 (18)	
c,1		0.0013 (2)	0.0006 (2)	-0.00535 (18)	
s,2		0.0003 (4)	0.0001 (3)	-0.0008 (2)	
c,2		0.0018 (4)	-0.0007 (3)	-0.0038 (2)	
O13		-0.2353 (2)	0.24376 (18)	0.54182 (15)	0.0258 (5)
s,1		0.0139 (3)	0.0145 (2)	0.01862 (19)	
c,1		0.0031 (3)	0.0023 (2)	-0.00192 (19)	
s,2		0.0002 (4)	-0.0002 (3)	0.0002 (3)	
c,2		0.0012 (4)	-0.0003 (3)	-0.0028 (3)	
O1w		0.2991 (6)	0.4617 (3)	0.3448 (4)	0.0890 (17)
s,1		-0.0173 (7)	-0.0003 (4)	0.0183 (5)	
c,1		0.0149 (7)	-0.0075 (4)	-0.0189 (5)	
s,2		0.0028 (11)	-0.0026 (7)	-0.0021 (7)	
c,2		0.0036 (9)	0.0007 (6)	-0.0033 (6)	
O2w		0.3184 (6)	0.1670 (7)	0.1090 (4)	0.0745 (18)
s,1		0.0095 (7)	-0.0338 (8)	-0.0105 (4)	
c,1		0.0341 (10)	-0.0488 (12)	-0.0052 (6)	
s,2		-0.0035 (9)	0.0137 (11)	0.0011 (6)	
c,2		-0.0147 (9)	0.0144 (10)	0.0024 (6)	
O3w		0.2867 (14)	0.4379 (9)	0.0478 (7)	0.129 (5)
s,1		-0.0071 (15)	-0.0143 (11)	-0.0075 (8)	
c,1		-0.0057 (16)	-0.0208 (11)	0.0102 (8)	

Rigid body parameters.

Cation	phi	chi	psi	xtrans	ytrans	ztrans
H ₂ DABCO ²⁺ 1	0	0	0	0.0076	0.0135	0.0404
				(3)	(3)	(3)
H ₂ DABCO ²⁺ 2	111.3 (2)	-19.69 (16)	-165.4 (4)	0.2118	-0.0644	0.0792
				(8)	(4)	(4)

Atoms in rigid body.

Atom	x	y	z
N1	0.0109	0.5895	0.727
N2	0.3272 (5)	0.6899 (5)	0.7908 (4)
C1	0.0458 (6)	0.7435 (5)	0.8104 (4)
C2	0.0952 (6)	0.5762 (6)	0.6241 (4)
C3	0.0767 (7)	0.5019 (6)	0.7838 (5)
C4	0.2369 (6)	0.8038 (5)	0.8469 (5)
C5	0.2872 (7)	0.6365 (8)	0.6623 (5)
C6	0.2711 (7)	0.5654 (6)	0.8260 (6)

4.2. Incommensurate $(\text{H}_2\text{DABCO})_2[\text{Mo}_8\text{O}_{26}]\cdot 4.66\text{H}_2\text{O}$, (II)

As already mentioned in §3, the structure of (II) resembles that of (I) except by its water-molecule and $\text{H}_2\text{DABCO}^{2+}$ content and ordering, which generate the incommensurability (see Fig. 4). The $[\text{Mo}_8\text{O}_{26}]^{4-}$ chains are nearly identical to those found in (I). In between those chains, the three independent $\text{H}_2\text{DABCO}^{2+}$ cations observed in (I) are condensed into one cation position in (II). That position is, however, split into two segments along the internal t coordinate, giving two different parallel-like and perpendicular-like orientations with similar site occupation factors (0.49 versus 0.51). With a small \mathbf{q} wavevector component along the \mathbf{a}^* axis (~ 0.06), the switching between the two orientations follows a rather long period, which can be put aside without loss of generality. We

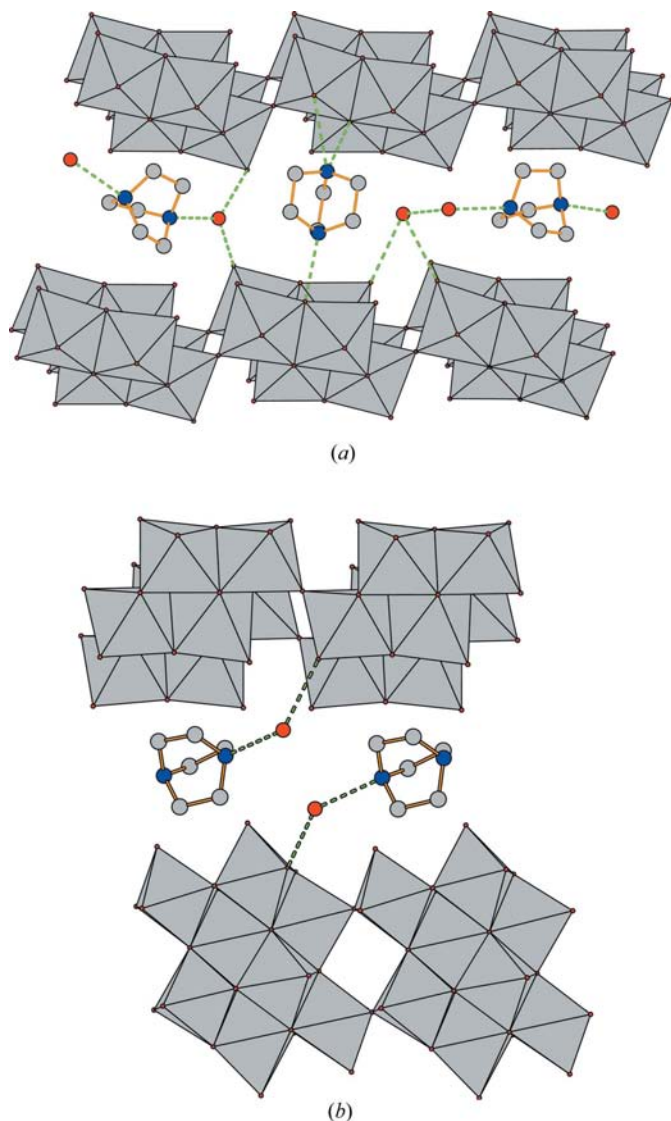


Figure 3
Illustration of the hydrogen-bond network in (a) (I) and (b) (III) (Fang *et al.*, 2004), pointing out the different parallel-like and perpendicular-like arrangements.

Table 4

Occupation factors, their Fourier series modulation terms and s.u. values for (II).

Fourier series†		
Atom	Wave sinus/cosinus, n	Occupation factor (p^v)
O3w	0	0.554 (16)
	s,1	-0.013 (10)
	c,1	0.008 (10)

† The p occupation modulation wave of an atom v is classically written as

$$p^v(x_4) = p_0^v + \sum_{n=1}^k p_{s,n}^v \sin(2\pi n x_4) + \sum_{n=1}^k p_{c,n}^v \cos(2\pi n x_4).$$

† Crenel functions†

Atom	Δ^v	$x_4^{0,v}$	Occupation (p_0^v)
O1w	0.932 (3)	0.866 (6)	1
O2w	0.855 (4)	0.067 (4)	1
$\text{H}_2\text{DABCO}^{2+}$ 1	0.487 (2)	0.0835 (8)	1
$\text{H}_2\text{DABCO}^{2+}$ 2	0.513 (2)	0.6136 (8)	1

† The p occupation modulation wave of an atom (H_2DABCO) v defined by a crenel function is given by

$$p^v(x_4) = p_0^v \times p_{\text{crenel}}^v(x_4)$$

with

$$p_{\text{crenel}}^v(x_4) = 1, \quad x_4 \in (x_4^{0,v} - \Delta^v/2, x_4^{0,v} + \Delta^v/2),$$

$$p_{\text{crenel}}^v(x_4) = 0, \quad x_4 \notin (x_4^{0,v} - \Delta^v/2, x_4^{0,v} + \Delta^v/2).$$

thus have, in a first approximation, rows of parallel-like or perpendicular-like $\text{H}_2\text{DABCO}^{2+}$ cations in between the POM anionic chains.

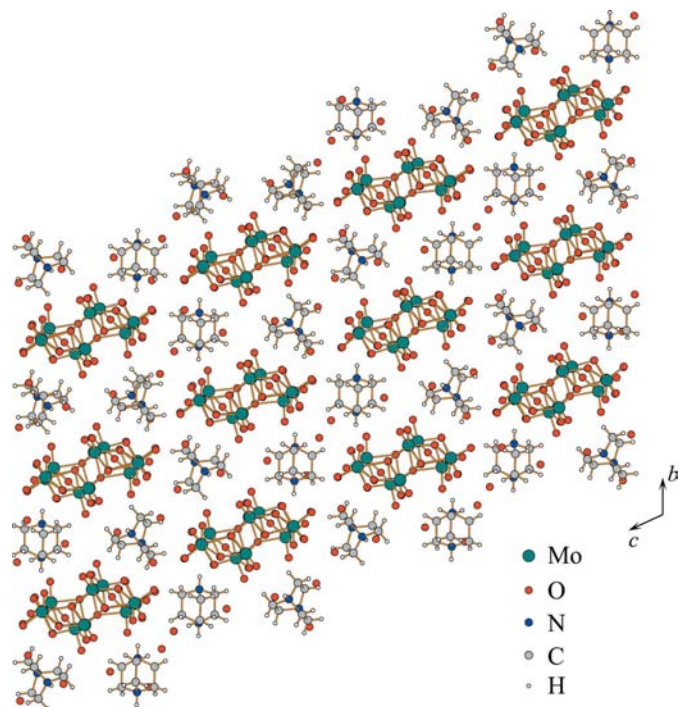


Figure 4
View of the incommensurate structure of (II), down the polyoxometalate anionic chain direction.

Table 5

Anisotropic displacement parameters U^{ij} (\AA^2), TLS parameters, their Fourier series modulation terms and their s.u. values for (II).

O-atom parameters are provided in the CIF.

Atom	Wave sinus/ cosinus,	U^{11}	U^{22}	U^{33}	U^{12}	U^{13}	U^{23}
Mo1		0.01765 (7)	0.02411 (8)	0.01514 (7)	0.00836 (6)	0.00484 (5)	0.00828 (6)
	s,1	-0.00118 (10)	0.00009 (11)	-0.00038 (10)	0.00031 (8)	-0.00047 (8)	0.00037 (8)
	c,1	-0.00125 (10)	-0.00077 (13)	-0.00198 (10)	-0.00084 (9)	-0.00076 (8)	-0.00225 (9)
Mo2		0.01580 (7)	0.02150 (7)	0.01672 (7)	0.00599 (5)	0.00213 (5)	0.00724 (6)
	s,1	-0.00049 (9)	0.00150 (9)	0.00119 (10)	0.00006 (7)	0.00129 (8)	0.00111 (8)
	c,1	-0.00106 (10)	-0.00170 (10)	-0.00069 (10)	-0.00090 (8)	-0.00063 (8)	-0.00173 (8)
Mo3		0.01236 (6)	0.01932 (7)	0.01823 (7)	0.00569 (5)	0.00447 (5)	0.01086 (6)
	s,1	0.00037 (8)	0.00086 (9)	0.00241 (11)	0.00035 (7)	0.00100 (8)	0.00177 (8)
	c,1	-0.00038 (9)	-0.00037 (8)	-0.00180 (10)	-0.00008 (7)	-0.00041 (7)	-0.00080 (7)
Mo4		0.01378 (6)	0.01632 (6)	0.01532 (7)	0.00663 (5)	0.00372 (5)	0.00822 (5)
	s,1	0.00016 (8)	0.00047 (8)	0.00225 (10)	0.00027 (7)	0.00057 (7)	0.00109 (7)
	c,1	-0.00099 (9)	-0.00073 (8)	-0.00033 (9)	-0.00088 (7)	-0.00061 (7)	-0.00046 (7)

The U modulation wave for the atomic displacement parameter of an atom ν is classically written as

$$U^{\nu}(x_4) = \sum_{n=1}^k f_{\lambda,s,n}^{\nu} \sin(2\pi n x_4) + \sum_{n=1}^v f_{\lambda,c,n}^{\nu} \cos(2\pi n x_4).$$

TLS parameters.

Rigid body	H ₂ DABCO ²⁺ 1	H ₂ DABCO ²⁺ 2	Rigid body	H ₂ DABCO ²⁺ 1	H ₂ DABCO ²⁺ 2
T^{11}	0.0099 (3)	0.0066 (3)	S^{11}	-0.0002 (3)	0.0023 (12)
T^{22}	0.0082 (2)	0.0177 (6)	S^{21}	-0.0019 (2)	-0.0052 (11)
T^{33}	0.00619 (19)	0.0217 (7)	S^{31}	-0.00151 (17)	-0.0260 (9)
T^{12}	0.0017 (2)	0.0010 (4)	S^{12}	-0.00082 (14)	0.0010 (3)
T^{13}	0.00096 (18)	0.0005 (4)	S^{22}	-0.0005 (3)	0.0027 (9)
T^{23}	0.00400 (17)	0.0036 (5)	S^{32}	0.00109 (17)	0.0005 (4)
L^{11}	0.0067 (3)	0.079 (2)	S^{13}	0.00028 (14)	0.0007 (3)
L^{22}	0.0034 (2)	0.0076 (5)	S^{23}	-0.00132 (16)	-0.0022 (5)
L^{33}	0.00213 (12)	0.0071 (3)	S^{33}	-0.0000 (3)	-0.0045 (11)
L^{12}	0.00249 (17)	0.0166 (8)			
L^{13}	0.00246 (13)	0.0222 (7)			
L^{23}	0.00145 (13)	0.0053 (4)			

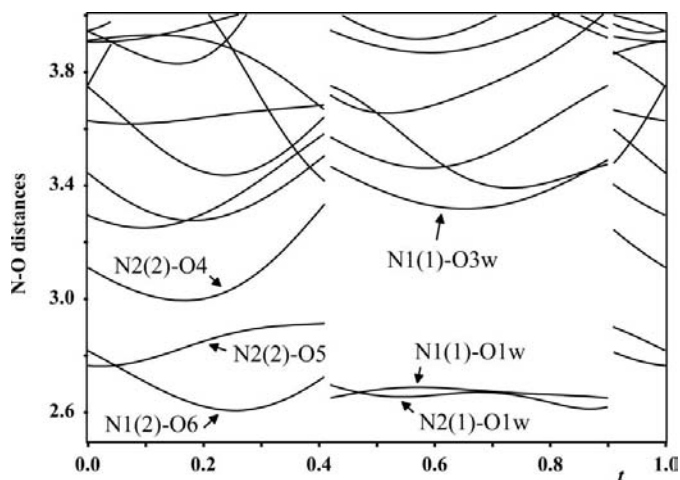


Figure 5

The N—O distances as a function of the internal t coordinate, illustrating the steadiness of the hydrogen bonds (shortest distances). Parallel-like H₂DABCO²⁺ cation with N1(1) and N2(1) and perpendicular-like H₂DABCO²⁺ cation with N1(2) and N2(2).

The parallel-like H₂DABCO²⁺ cations establish hydrogen bonds with the water molecules, whereas the perpendicular-like H₂DABCO²⁺ cation are linked to the [Mo₈O₂₆]⁴⁻ chains *via* similar hydrogen bonds (see Fig. 5). Since the parallel-like H₂DABCO²⁺ cations are slightly tilted, two successive H₂DABCO²⁺ cations along the a axis are not linked to the same water molecule. In other words, a water molecule never links two H₂DABCO²⁺ cations but links one H₂DABCO²⁺ cation either to an anionic chain or to another water molecule. Along the chain direction, in between consecutive perpendicular-like H₂DABCO²⁺ cations, are located water molecules (O3w) which are only connected to the inorganic chains. The shortest C—O distance between the parallel-like H₂DABCO²⁺ cation and the polyoxometalate chain is calculated at 2.91 Å for the parallel-like cation and compares well with the shortest C—O distance of 2.95 Å calculated for (I), whatever the cation orientation. In contrast, the shortest C—O distance between the perpendicular-like H₂DABCO²⁺ cation and the polyoxometalate chain is 2.655 Å. This too-short distance is in fact only apparent since the perpendicular-like H₂DABCO²⁺ cation is highly rotationally disordered, as revealed by the large L^{ij} libration and S^{ij} screw correlation tensor components, the real distances being probably of the order of those observed for the parallel-like cation (see Fig. 6). This rotational

disorder is probably to be linked to the observed disorder of the water molecule, Ow3, with a site occupancy factor of ~50%.

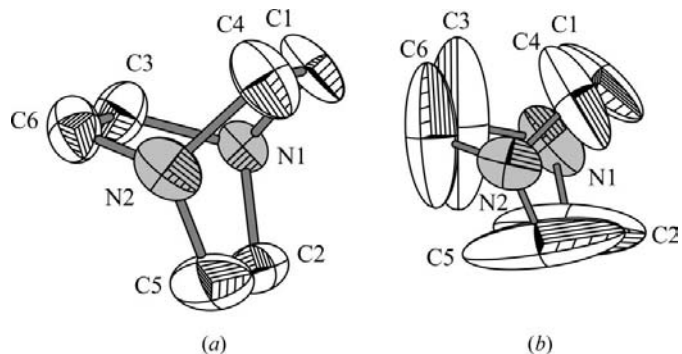


Figure 6

Parallel-like (a) and perpendicular-like (b) H₂DABCO²⁺ cations, illustrating the high rotational disorder for the latter cation. Displacement ellipsoids are drawn at the 50% probability level.

5. Concluding remarks

In this report, we have described the syntheses and crystal structure determinations of two new organic–inorganic hybrid compounds based on polyoxometalates, commensurate $(\text{H}_2\text{DABCO})_2[\text{Mo}_8\text{O}_{26}] \cdot 4\text{H}_2\text{O}$, (I), and incommensurate $(\text{H}_2\text{DABCO})_2[\text{Mo}_8\text{O}_{26}] \cdot 4.66\text{H}_2\text{O}$, (II). Their structural similarity has been demonstrated, their difference being predominantly related to the water molecule content. Interestingly, a complex hydrogen-bond network has been observed, not only between the $\text{H}_2\text{DABCO}^{2+}$ cations and the water molecules or between the $[\text{Mo}_8\text{O}_{26}]^{4-}$ chains and the water molecules, as in monoclinic $(\text{H}_2\text{DABCO})_2[\text{Mo}_8\text{O}_{26}] \cdot 4\text{H}_2\text{O}$, (III), but also between some of the $\text{H}_2\text{DABCO}^{2+}$ cations and the polyoxometalate chains. Those latter hydrogen bonds are supposed to be a prerequisite for their photochromic properties. However, in spite of the occurrence of hydrogen bonds between the $\text{H}_2\text{DABCO}^{2+}$ cations and the $[\text{Mo}_8\text{O}_{26}]^{4-}$ chains, none of the three $(\text{H}_2\text{DABCO})_2[\text{Mo}_8\text{O}_{26}] \cdot x\text{H}_2\text{O}$ materials is photochromic. Therefore, we may conclude that the existence of $\text{H} \cdots \mu_2\text{-O}$ connections is a required but not sufficient factor for inducing photochromism. This point will be highlighted in a coming paper dedicated to DABCO/molybdate systems.

Vaclav Petricek was able to participate in this work thanks to support from the Grant Agency of the Czech Republic, grant 202/06/0757.

References

- Brandenburg, K. (2001). *DIAMOND*. Version 3. Crystal Impact GbR, Bonn, Germany.
- Burla, M. C., Caliandro, R., Camalli, M., Carrozzini, B., Cascarano, G. L., De Caro, L., Giacovazzo, C., Polidori, G. & Spagna, R. (2005). *J. Appl. Cryst.* **38**, 381–388.
- Chakrabarti, S. & Natarajan, S. (2002). *Cryst. Growth. Des.* **2**, 333–335.
- Coué, V., Dessapt, R., Bujoli-Doeuff, M., Evain, M. & Jobic, S. (2006). *Inorg. Chem.* Submitted.
- Duisenberg, A. J. M., Kroon-Batenburg, L. M. J. & Schreurs, A. M. M. (2003). *J. Appl. Cryst.* **36**, 220–229.
- Evain, M. (1992). *U-Fit*. Institut des Matériaux Jean Rouxel, Nantes, France.
- Fang, R.-Q., Zhang, X.-M., Wu, H.-S. & Ng, S. W. (2004). *Acta Cryst.* **E60**, m359–m361.
- Herrendorf, W. (1993). *HABITUS*. PhD dissertation, University of Karlsruhe, Germany.
- Katsoulis, D. E. (1998). *Chem. Rev.* **98**, 359–387.
- Mizuno, N. & Misono, M. (1998). *Chem. Rev.* **98**, 199–218.
- Petricek, V., Dusek, M. & Palatinus, L. (2000). *JANA2000*. Institute of Physics, Academy of Sciences of the Czech Republic, Prague, Czech Republic.
- Petricek, V., van der Lee, A. & Evain, M. (1995). *Acta Cryst.* **A51**, 529–531.
- Rhule, J. T., Hill, C. L., Jude, D. A. & Schinazi, R. F. (1998). *Chem. Rev.* **98**, 327–358.
- Stoe & Cie (1996). *X-SHAPE*. Version 1.02. Stoe & Cie, Darmstadt, Germany.
- Thorn, K. J., Narducci Sarjeant, A. & Norquist, A. J. (2005). *Acta Cryst.* **E61**, m1665–m1667.
- Yamase, T. (1998). *Chem. Rev.* **98**, 307–325.